

## Determination of electron escape depth in ultrathin silicon oxide

H. Nohira<sup>a)</sup> and H. Okamoto

*Department of Electrical & Electronic Engineering, Musashi Institute of Technology, 1-28-1 Tamazutsumi, Setagaya-ku, Tokyo 158-8557, Japan*

K. Azuma and Y. Nakata

*Advanced LCD Technologies Development Center Co. Ltd., 292 Yoshida-cho, Totsuka-ku, Yokohama, 244-0817, Japan*

E. Ikenaga and K. Kobayashi

*JASRI/SPring-8, Mikaduki-cho, Sayo-gun, Hyogo 679-5198, Japan*

Y. Takata and S. Shin

*RIKEN/SPring-8, Mikaduki-cho, Sayo-gun, Hyogo 679-5148, Japan*

T. Hattori

*Research Center for Silicon Nano-Science, Advanced Research Laboratories, Musashi Institute of Technology, 8-15-1 Todoroki, Setagaya-ku, Tokyo 158-0082, Japan*

(Received 23 September 2004; accepted 28 December 2004; published online 16 February 2005)

Using the high-brilliance synchrotron radiation at SPring-8, we determined the electron escape depths in approximately 1-nm-thick low-temperature oxide layers, which were formed on Si(100) at 300 °C using three kinds of atomic oxygen and that in approximately 1-nm-thick thermally grown oxide layer formed in 1 Torr dry oxygen at 900 °C by measuring angle-resolved Si 2*p* photoelectron spectra at the photon energy of 1050 eV. The results indicated that the electron escape depths in the three kinds of low-temperature oxide layers were 18%–24% smaller than that in the thermally grown oxide layer. Furthermore, the electron escape depth in the thermally grown oxide layer, whose thickness was close to that of the structural transition layer, was 7% smaller than that in bulk SiO<sub>2</sub>. © 2005 American Institute of Physics. [DOI: 10.1063/1.1868066]

The electron escape depth in silicon oxide layer and that in silicon used for the determination of silicon oxide thickness by x-ray photoelectron spectroscopy have been determined by measuring the number of x-ray excited photoelectrons arising from silicon oxide layer and that arising from silicon as a function of thickness of silicon oxide layer.<sup>1,2</sup> However, such method cannot be applied to the oxide layer with the thickness on the order of 1 nm, which mostly determines the quality of a SiO<sub>2</sub>/Si interfacial transition layer. One of our goals is to establish a low-temperature oxidation process for the gate insulator of thin-film transistors on glass or plastic substrates. Radical oxidation is one of the most effective ways to conduct an oxidation reaction at low temperature. We evaluated three approaches for effectively generating oxygen radicals. Photo-oxidation uses a xenon excimer lamp producing 172 nm wavelength light, which has a photon energy sufficient to selectively obtain O(1D) radicals and lower than the SiO<sub>2</sub> band gap in order to suppress defect production at the SiO<sub>2</sub>/Si interface. Plasma-enhanced oxidation, which is further enhanced by adding a rare gas such as Kr, is also effective for obtaining high-density oxygen radicals. In the present letter the method of determining the electron escape depths in ultrathin silicon oxide layers by measuring angle-resolved Si 2*p* photoelectron spectra is proposed and the electron escape depths in low-temperature oxides formed at 300 °C using three kinds of atomic oxygen are found to be clearly different from that in thermally grown oxide layer formed at 900 °C using molecular oxygen.

On a vicinal Si(100) 0.01° surface, a 0.72-nm-thick oxide layer was formed at 300 °C by using atomic oxygen produced in a krypton-mixed oxygen (Kr:O<sub>2</sub>=97:3) plasma excited by microwave radiation (2.45 GHz); this layer is referred to as Kr/O<sub>2</sub> plasma oxide hereafter.<sup>3</sup> On the same kind of surface, a 0.86-nm-thick oxide layer was formed at 300 °C by using atomic oxygen produced in an oxygen plasma excited by microwave radiation (2.45 GHz); this layer is referred to as O<sub>2</sub> plasma oxide hereafter.<sup>3</sup> Finally, on a third sample with the same kind of surface, a 0.85-nm-thick oxide layer, referred to as photo-oxide hereafter, was formed at 300 °C by using atomic oxygen produced by exciting molecular oxygen with a xenon excimer lamp. As a reference, a high-quality 1.25-nm-thick silicon oxide layer, referred to as thermal oxide hereafter, was formed in dry oxygen at 900 °C on another vicinal Si(100) 0.01° surface covered with a 0.3-nm-thick pre-oxide layer formed in dry oxygen at 300 °C.<sup>4</sup> The thicknesses of SiO<sub>2</sub> layers were evaluated from the angle-resolved Si 2*p* photoelectron spectra discussed and the thicknesses of compositional transition layers were evaluated from the measurement of Si 2*p* photoelectron spectra at photoelectron take-off angle of 55°, where the effect of elastic scattering can be effectively neglected.<sup>5</sup> Using electron energy analyzer ESCA-200 angle-resolved 1050 eV photons' excited Si 2*p* photoelectron spectra were measured with energy resolution of 100 meV at soft-x ray undulator beam line (BL27SU) of the Super Photon Ring 8 GeV (SPring-8).

Figure 1 shows 1050 eV photons' excited Si 2*p*<sub>3/2</sub> photoelectron spectra arising from Kr/O<sub>2</sub> plasma oxide, O<sub>2</sub> plasma oxide, photo-oxide and thermal oxide with photo-

<sup>a)</sup>Electronic mail: nohira@ee.musashi-tech.ac.jp

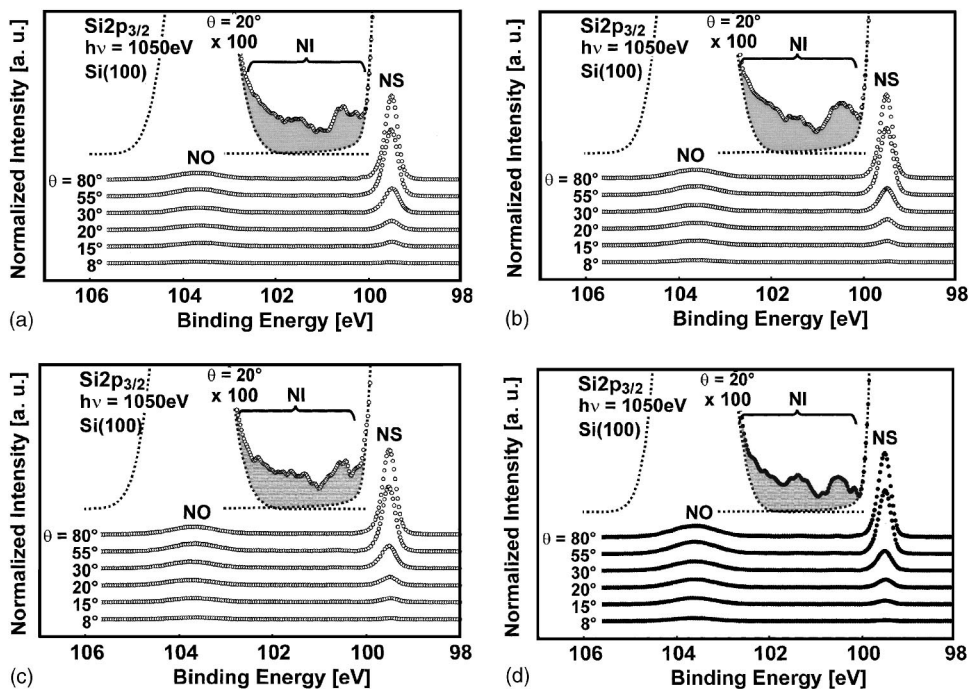


FIG. 1. 1050 eV photons' excited Si  $2p_{3/2}$  photoelectron spectra with photoelectron take-off angle  $\theta$  as a parameter measured for (a) the Kr/ $O_2$  plasma oxide, (b) the  $O_2$  plasma oxide, (c) the photo-oxide, and (d) the thermal oxide, which were formed on Si(100) surfaces.

electron take-off angle  $\theta$  as a parameter. Here, the refraction of the electron wave at vacuum/ $SiO_2$  interface was taken into account.<sup>6</sup> With decreasing  $\theta$ , the Si  $2p$  photoelectron spectral intensities arising from the Si substrate decreased. This confirmed that the Si substrates were, in fact, covered with silicon oxide layers. Furthermore, the Si  $2p_{3/2}$  spectral intensity, NI, arising from the compositional transition layer consisting of intermediate oxidation states of Si measured at photoelectron take-off angle of  $20^\circ$  is indicated by the shaded region in each graph. The amounts of NI are 0.759 ML for Kr/ $O_2$  plasma oxide, 0.865 ML for  $O_2$  plasma oxide, 0.881 ML for photo-oxide, and 0.835 ML for thermal oxide, respectively. Here, 1 ML expresses  $6.80 \times 10^{14} \text{ cm}^{-2}$ .

The dependencies of NI/NO on  $\theta$  measured for three kinds of low-temperature oxide layers formed on Si(100) are compared with that measured for thermal oxide in Fig. 2. Here, NO represents the Si  $2p$  spectral intensity arising from  $SiO_2$ . The dependence of NI/NO on  $\theta$  can be expressed as a

function of the electron escape depth  $\Lambda_O$  in the  $SiO_2$  layer by the following equation. Here, it should be noted that the effect of photoelectron diffraction on the dependence of NI/NO on  $\theta$  does not have to be taken into account, because the oxide layers are in amorphous states,

$$\frac{NI}{NO} = \frac{n_t \Lambda_t \sin \theta \left\{ 1 - \exp\left(-\frac{t}{\Lambda_t \sin \theta}\right) \right\}}{n_o \Lambda_o \sin \theta \left\{ \exp\left(\frac{d}{\Lambda_o \sin \theta}\right) - 1 \right\}}. \quad (1)$$

Here,  $n_O$  and  $n_t$ ,  $d$  and  $t$ , and  $\Lambda_t$  denote the densities of silicon atoms in the  $SiO_2$  layer and the compositional transition layer, the thicknesses of the  $SiO_2$  layer and the compositional transition layer, and the electron escape depth in the compositional transition layer, respectively. The following relation between  $\Lambda_O$  and  $d$  should be satisfied.

$$\frac{NO}{NS} = \frac{n_o \Lambda_o \left\{ \exp\left(\frac{d}{\Lambda_o \sin \theta}\right) - 1 \right\}}{n_s \Lambda_s \exp\left(-\frac{t}{\Lambda_t \sin \theta}\right)}. \quad (2)$$

Here,  $\Lambda_s$  represents the electron escape depth in the silicon substrate. The value of  $\Lambda_s$  (1.59 nm) was calculated from the escape depth (2.11 nm) of Si  $2p$  photoelectrons in silicon excited by Al  $K\alpha$  radiation,<sup>2</sup> by considering the dependence of the electron escape depth on the kinetic energy of the electrons.<sup>7</sup> The following relation between  $\Lambda_t$  and  $t$  should also be satisfied,

$$\frac{NI}{NS} = \frac{n_t \Lambda_t \left\{ \exp\left(\frac{t}{\Lambda_t \sin \theta}\right) - 1 \right\}}{n_s \Lambda_s}. \quad (3)$$

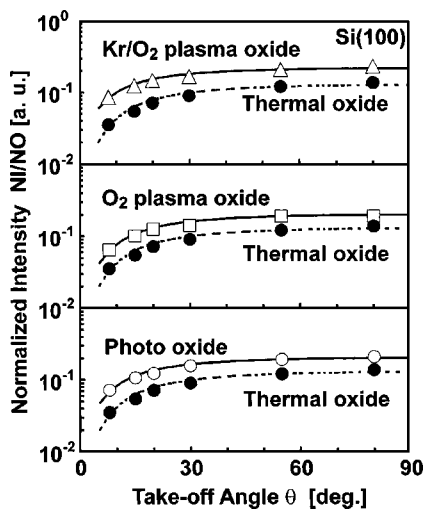


FIG. 2. Dependence of NI/NO on  $\theta$  for (a) Kr/ $O_2$  plasma oxide, (b)  $O_2$  plasma oxide, and (c) photo-oxide. As a reference, the dependence of NI/NO on  $\theta$  for the thermal oxide is also shown.

TABLE I. Electron escape depths in low-temperature oxides.

	Kr/O <sub>2</sub> plasma oxide	O <sub>2</sub> plasma oxide	Photo-oxide	Thermal oxide
$\Lambda_0$ (nm)	2.04	2.06	2.19	2.67

The values of  $\Lambda_0$  for the four kinds of oxides were determined by least-squares fitting, shown by the solid and dashed curves in Fig. 2, which were calculated using Eq. (1), with the experimental data. Here, we assumed that  $n_O$  was the value for bulk SiO<sub>2</sub>, and that  $n_t = (n_s + n_O)/2$  and  $\Lambda_t = (\Lambda_s + \Lambda_O)/2$ . We used values of  $5 \times 10^{28} \text{ cm}^{-2}$  for  $n_s$  and  $2.28 \times 10^{28} \text{ cm}^{-2}$  for  $n_O$ .<sup>8</sup> The resulting values of  $\Lambda_0$  are listed in Table I. As shown in Table I, the electron escape depth (2.67 nm) in thermal oxide, whose thickness (1.25 nm) was comparable to the thickness of the structural transition layer consisting of SiO<sub>2</sub>,<sup>9</sup> was smaller than 2.86 nm, whose value calculated from the escape depth (3.80 nm)<sup>10</sup> of Si 2*p* photoelectrons excited by Al *K* $\alpha$  radiation in thermally grown bulk SiO<sub>2</sub> by considering the dependence of the electron escape depth on the kinetic energy of the electrons.<sup>7</sup> This must be correlated with the observation that the density of the structural transition layer is approximately 5% larger than that of bulk SiO<sub>2</sub>.<sup>11</sup> The electron escape depths in three kinds of low temperature oxides listed in Table I are 18%–24% smaller than that in thermal oxide. Because the difference between the densities of low-temperature oxide and thermal oxide is nearly 5%, the difference between the electron escape depths in each type of oxide cannot be ascribed to the density difference; rather, it may be ascribed to the difference in the electron scattering mechanisms. Specifically, because the fraction of oxygen atoms that are not incorporated in the oxide network may be larger in low-temperature oxide than in thermal oxide, the scattering frequency of electrons may be larger in the low-temperature oxide, resulting in a smaller electron escape depth as compared to that in the thermal oxide. Furthermore, it should be noted that the electron escape depth in the

Kr/O<sub>2</sub> plasma oxide and in the O<sub>2</sub> plasma oxide was 6% smaller than that in the photo-oxide.

In conclusion, the electron escape depths in three kinds of ultrathin low-temperature-oxide and that in ultrathin thermal oxide were determined from angle-resolved Si 2*p* photoelectron spectra. We found that the electron escape depths in the low-temperature oxide layers were 18%–24% smaller than that in the thermal oxide. The results also indicated that the electron escape depth in the thermal oxide, whose thickness was close to that of the structural transition layer, was 7% smaller than that in bulk SiO<sub>2</sub>.

The synchrotron radiation experiments were performed at SPring-8 with the approval of Japan Synchrotron Radiation Research Institute as a Nanotechnology Support Project of The Ministry of Education, Culture, Sports, Science and Technology. This work was partially supported by the Ministry of Education, Science, Sports and Culture through a Grant-in-Aid for Scientific Research (A) (No. 32678), and partially by the Ministry of Economy, Trade and Industry and the New Energy and Industrial Technology Development.

<sup>1</sup>R. Flitsch and S. I. Raider, *J. Vac. Sci. Technol.* **12**, 305 (1975).

<sup>2</sup>Z. H. Lu, J. P. McCaffrey, B. Brar, G. D. Wilk, R. M. Wallace, L. C. Feldman and S. P. Tay, *Appl. Phys. Lett.* **71**, 2764 (1997).

<sup>3</sup>M. Goto, K. Azuma, T. Okamoto, and Y. Nakata, *Jpn. J. Appl. Phys., Part 1* **42**, 7033 (2003).

<sup>4</sup>T. Hattori, K. Takahashi, M. B. Seman, H. Nohira, K. Hirose, N. Kamakura, Y. Takata, S. Shin, and K. Kobayashi, *Appl. Surf. Sci.* **212–213**, 547 (2003).

<sup>5</sup>T. Hattori, K. Hirose, H. Nohira, K. Takahashi, and T. Yagi, *Appl. Surf. Sci.* **144–145**, 297 (1999).

<sup>6</sup>D.-A. Luh, T. Miller, and T.-C. Chiang, *Phys. Rev. Lett.* **79**, 3014 (1997).

<sup>7</sup>M. P. Seah and W. A. Dench, *Surf. Interface Anal.* **1**, 2 (1979).

<sup>8</sup>M. F. Hochella Jr. and A. H. Carim, *Surf. Sci.* **197**, L260 (1988).

<sup>9</sup>K. Hirose, H. Nohira, T. Koike, K. Sakano, and T. Hattori, *Phys. Rev. B* **59**, 5617 (1999).

<sup>10</sup>K. Takahashi, K. Hirose, H. Nohira, and T. Hattori, *Appl. Phys. Lett.* **83**, 3422 (2003).

<sup>11</sup>Y. Sugita, S. Watanabe, N. Awaji, and S. Komiya, *Appl. Surf. Sci.* **100/101**, 268 (1996).